COMET

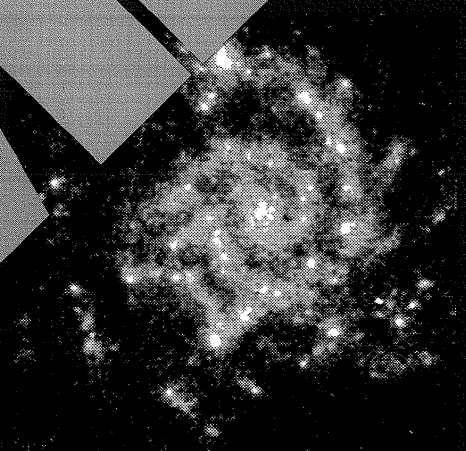

The NASA STI Program ... in Profile

Since its founding, NASA has been dedicated to ensuring U.S. leadership in aeronautics and space science. The NASA Scientific and Technical Information (STI) Program plays an important part in helping NASA maintain its leadership role.

The NASA STI Program provides access to the NASA STI Database, the largest collection of aeronautical and space science STI in the world. The Program is also NASA's institutional mechanism for disseminating the results of its research and development activities.

A number of specialized services help round out the Program's diverse offerings, including creating custom thesauri, translating material to or from 34 foreign languages, building customized databases, organizing and publishing research results.

For more information about the NASA STI Program, you can:

- **Phone** the NASA Access Help Desk at (301) 621-0390
- **Fax** your question to NASA Access Help Desk at (301) 621-0134
- Send us your question via the **Internet** to help@sti.nasa.gov
- **Write to:**

  NASA Access Help Desk
  NASA Center for AeroSpace Information
  800 Elkridge Landing Road
  Linthicum Heights, MD 21090-2934

56P. CR

IN-27831

JPL PUBLICATION 86-19

A Portable Spectrometer for Use From 5 to 15 Micrometers

Gordon Hoover
Anne B. Kahle

July 1, 1986

National Aeronautics and
Space Administration

Jet Propulsion Laboratory
California Institute of Technology
Pasadena, California

JPL PUBLICATION 86-19

A Portable Spectrometer for Use From 5 to 15 Micrometers

Gordon Hoover
Anne B. Kahle

July 1, 1986

National Aeronautics and
Space Administration

Jet Propulsion Laboratory
California Institute of Technology
Pasadena, California

The research described in this publication was carried out by the Jet Propulsion Laboratory, California Institute of Technology, under a contract with the National Aeronautics and Space Administration.

ACKNOWLEDGEMENTS

This instrument has been developed over the past several years by many individuals under a contract with the Land Processes Branch of the National Aeronautics and Space Administration. In the early phases of planning and construction, Alexander F. H. Goetz, Tetsuo Ozawa, LLoyd Back, Guy Morrison, Colin Mahoney, and Anne Kahle, all of the Jet Propulsion Laboratory, made substantial contributions. In addition, much of the detailed design and construction work was carried out under a contract with the Santa Barbara Research Center, a division of the Hughes Aircraft Co.

Early field testing, which was carried out mainly by Richard Machida and Anne Kahle, made it clear that there remained some obstacles to be overcome with regard to the stability and calibration of the instrument. Gordon Hoover, with the assistance of Mary Jane Bartholomew, undertook a thorough reappraisal of the operating procedures and ways were found around the obstacles. Stanley Schultz developed the computer software for testing and calibrating the instrument and for processing the data. The sheer physical exertion involved in field operations requires that we acknowledge the contribution to this side of the effort by Stan Schultz, Anne Kahle, Gordon Hoover, Leon Maldonado, Mary Jane Bartholomew, Mike Abrams, Elsa Abbott, Cindy Inouye, Alan Gillespie, Frank Palluconi, and other long-suffering members of the Geologic Remote Sensing Group.

We are grateful to James Conel, Frank Palluconi, and Harold Lang, who read this report prior to publication and made numerous suggestions for its improvement.

ABSTRACT

A field portable spectrometer suitable for collecting data relevant to remote sensing applications in the 8 to 12 micrometer atmospheric window has been built at the Jet Propulsion Laboratory. The instrument employs a single cooled HgCdTe detector and a continuously variable filter wheel analyzer. The spectral range covered is 5 to 14.5 micrometers and the resolution is approximately 1.5 percent of the wavelength.

A description of the hardware is followed by a discussion of the analysis of the spectral data leading to finished emissivity and radiance spectra. A section is devoted to the evaluation of the instrument performance with respect to spectral resolution, radiometric precision, and accuracy. Several examples of spectra acquired in the field are included.

CONTENTS

CONTENTS (Contd)

CONTENTS (Contd)

Figures

SECTION 1

INTRODUCTION

A field-portable spectrometer for operation in the 5 to 14.5 micrometer region of the infrared spectrum has been built at the Jet Propulsion Laboratory. This instrument, the Portable Field Emission Spectrometer (PFES), was built for the purpose of measuring the ambient spectral thermal emission of geologic materials in situ, avoiding the disturbance of the natural setting which occurs when samples have to be transported to the laboratory. The instrument employs a filter wheel analyzing element and a cooled HgCdTe detector.

Spectra provided by this instrument will aid in the interpretation of data acquired by the airborne Thermal Infrared Multispectral Scanner (TIMS) [Kahle and Goetz, 1983 (Reference 1-1)]. The instrument will also be used to help define the design requirements (spectral resolution, band positions, and NEΔT) for future remote sensing instruments to be operated in this wavelength region.

Some years before the PFES was built, Goetz of JPL's Geologic Remote Sensing Group had developed a portable spectrometer for the 0.4 to 2.5 micrometer region, designated the PFRS, for Portable Field Reflectance Spectrometer [Goetz, et al, 1975 (Reference 1-2)]. Its purpose, like that of the instrument described here, was mainly to gather data that would be of help in planning remote sensing experiments and to make it possible to compare the resulting data with measurements made at the sites themselves. The PFES was designed to be compatible with this already-existing system, making use of the same data recorder and power supplies.

Here, we shall discuss the complete PFES system, breaking it down into its logical subsystems. Also we will describe our methods of analyzing the data and present a few sample spectra.

Using and maintaining the instrument over the past several years has led to a number of simplifications in the hardware and some modifications in the operating procedures. However, the period of rapid evolution commonly experienced with prototype systems is now in the past.

1.1 GENERAL DESCRIPTION

The complete spectrometer system consists of two main parts, the sensor head and the data recorder. Each of these is mounted on a packframe for easy carrying. Other parts of the system include a gas bottle, signal monitoring box, reference blackbody, and connecting cables. Figure 1-1 shows the system in use at a field site.

The sensor head (Figure 1-2), contains the optics, the detector, and preamplifiers. During operation, the sensor head is connected by a hose to a tank that supplies high pressure argon gas for cooling the detector. The head and its pack frame weigh 11.4 kg (25 lb). The tank of argon weighs about 6.8 kg (15 lb).

The data recorder consists of a number of electronic subassemblies attached to an aluminum sheet, which is bolted to a pack frame. A fiberglass cover provides structural rigidity and protection. Contained in the data recorder are the battery, digital cassette tape recorder, signal processing circuitry, logic circuits pertaining to data recording and sequencing the spectral scanner, and power converters for supplying the various voltages needed. Operator controls are located on the data recorder box and on a small monitor head connected to the data recorder by a cable. The data recorder weighs approximately 18.2 kg (40 lb).

The head and the data recorder are connected together by a multi-conductor electric cable over which the spectral data are transmitted as analog voltages. The cable also carries sample identification codes in parallel digital form, chopper phase signals, and power of various voltages.

Figure 1-1. Spectrometer Deployed in the Field

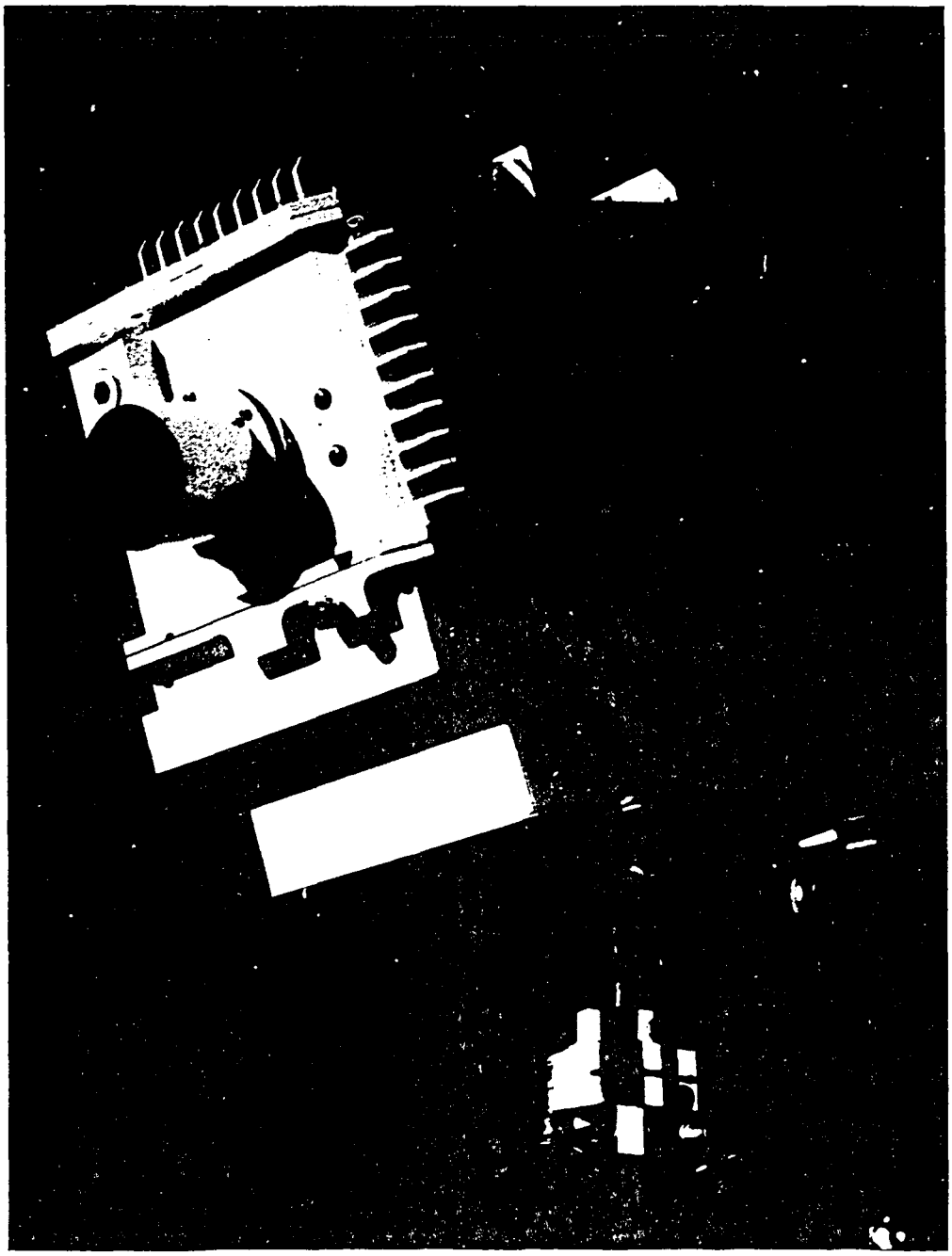

Figure 1-2. Sensor Head

SECTION 2

SENSOR HEAD

The outer case of the head is a sturdy box, milled out of a solid block of aluminum, and sealed against moisture and dust by O-rings. The functional parts of the sensor head are illustrated in Figure 2-1. Its key elements will next be described, starting with the optics.

2.1 OPTICS

A scale drawing of the optical train appears in Figure 2-2, and specifications of the elements are given in Table 2-1. All lenses are of optical grade germanium and coated on both sides with a multilayer antireflection coating, with a minimum transmission per element of 92 percent for the 5 to 14.5 micrometer range. The front surface of element 1 was coated with a monolayer of ZnO which was considered more abrasion resistant than the multilayer coating.

The detector is housed in a small dewar behind a window of uncoated Irtran 2. (Irtran is a registered trademark of the Eastman Kodak Co., who sells a series of infrared optical materials under the name. The different Irtrans are hot-pressed polycrystalline compacts consisting of varying ratios of MgF , ZnS, CdF , ZnSe, MgO, and CdTe.) The 1 by 3.5 millimeter sensitive area of the detector is imaged by lenses four and five onto the filter wheel, defining the spectral extent of a sample. Lenses two and three reimage the detector onto the plane of the chopper mirror. The focal plane of lens one coincides with lens two which is the target defining aperture resulting in a 15 degree circular field of view. The focus is set for a distance of one meter although the working distance is not critical because most geologic targets of interest present a homogeneous field extending beyond the edges of the field of view.

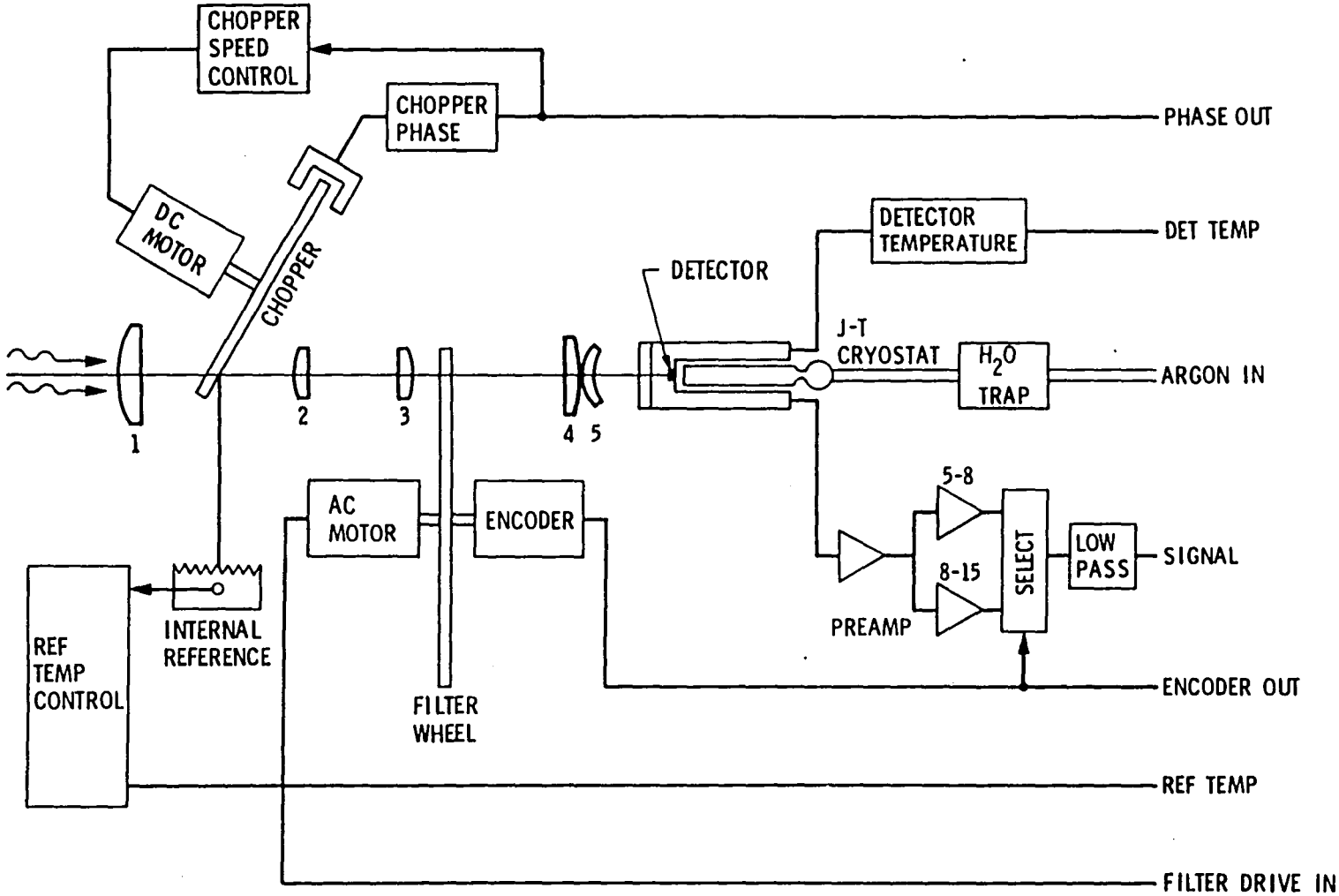

Figure 2-1. Functional Diagram of the Sensor Head

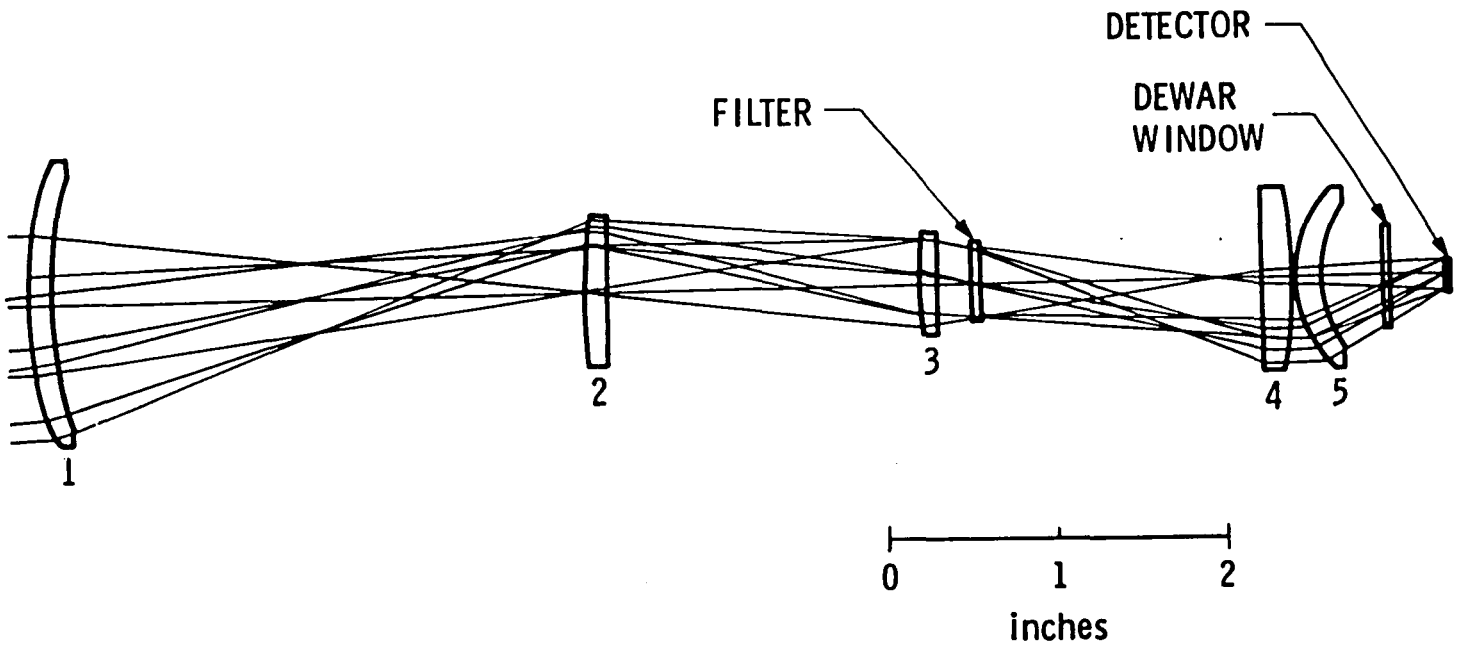

Figure 2-2. Optics

Table 2-1. Optical Specifications*

Element	R1	R2	T	Clear Aperture 1	Clear Aperture 2
1	2.1381	2.6770	0.1575	1.5383	1.4663
Air Space			1.4753		
Aperture Stop			0	0.3984	
Air Space			1.5672		
2	2.4060	14.6470	0.1271	0.8073	0.7992
Air Space			1.7566		
3	1.7430	4.7470	0.1118	0.5285	0.5055
Air Space			0.1969		
Filter	Inf.	Inf.	0.0550	0.3976	0.3937
Air Space			1.6085		
4	-17.7480	-2.8470	0.1772	0.9376	0.9692
Air Space			0.0197		
5	0.7080	0.7490	0.1495	0.9354	0.8153
Air Space			0.3543		
Window	Inf.	Inf.	0.0394	0.5265	0.5161
Vacuum			0.3085		
Detector					

*Dimensions are given in inches.

Note: R1, R2 are front and rear surface radii of curvature. (+) for center to the right, (-) for center to the left. T is the thickness of the element on the optic axis or the separation of elements.

Clear Aperture 1 and Clear Aperture 2 are the unobstructed diameters of the 1st and 2nd surfaces of element.

2.2 FILTER WHEEL

The analyzing element of the spectrometer is a filter wheel containing three filter segments of the continuously variable multilayer interference type. Figure 2-3 shows a view of the filter wheel and Table 2-2 lists specifications of the three segments. Each filter segment is sandwiched with a blocking filter that limits transmission outside its range to less than 0.5 percent.

The weakness of emission from natural surfaces in the 2.5 to 4.5 micrometer region and the confusion arising from the competition of reflected solar radiation has led us to restrict our attention, to date, to the second and third segments only, covering the region from 4.4 to 14.5 micrometers.

During the scanning of a spectrum, the filter wheel is driven at a constant speed by a small ac motor. An absolute shaft encoder is mounted on the filter wheel shaft and transmits wavelength information to the data recorder. One complete revolution is broken into 512 equal increments, each of which gives rise to a distinct nine bit gray code. The output of the shaft encoder also triggers sampling and recording, and controls the sequence of operations during a scan.

The use of a filter wheel lends the system a simplicity and ruggedness that would be more difficult to achieve with an analyzer based on diffraction gratings. A continuously variable filter has a somewhat limited spectral resolution but it is adequate for most geological applications and is the logical choice here. Moreover, with a filter it is much easier to achieve the high throughput needed for measuring the relatively weak emission from ambient temperature targets. This is mainly because of the more restricted area of the entrance slit of a grating spectrometer.

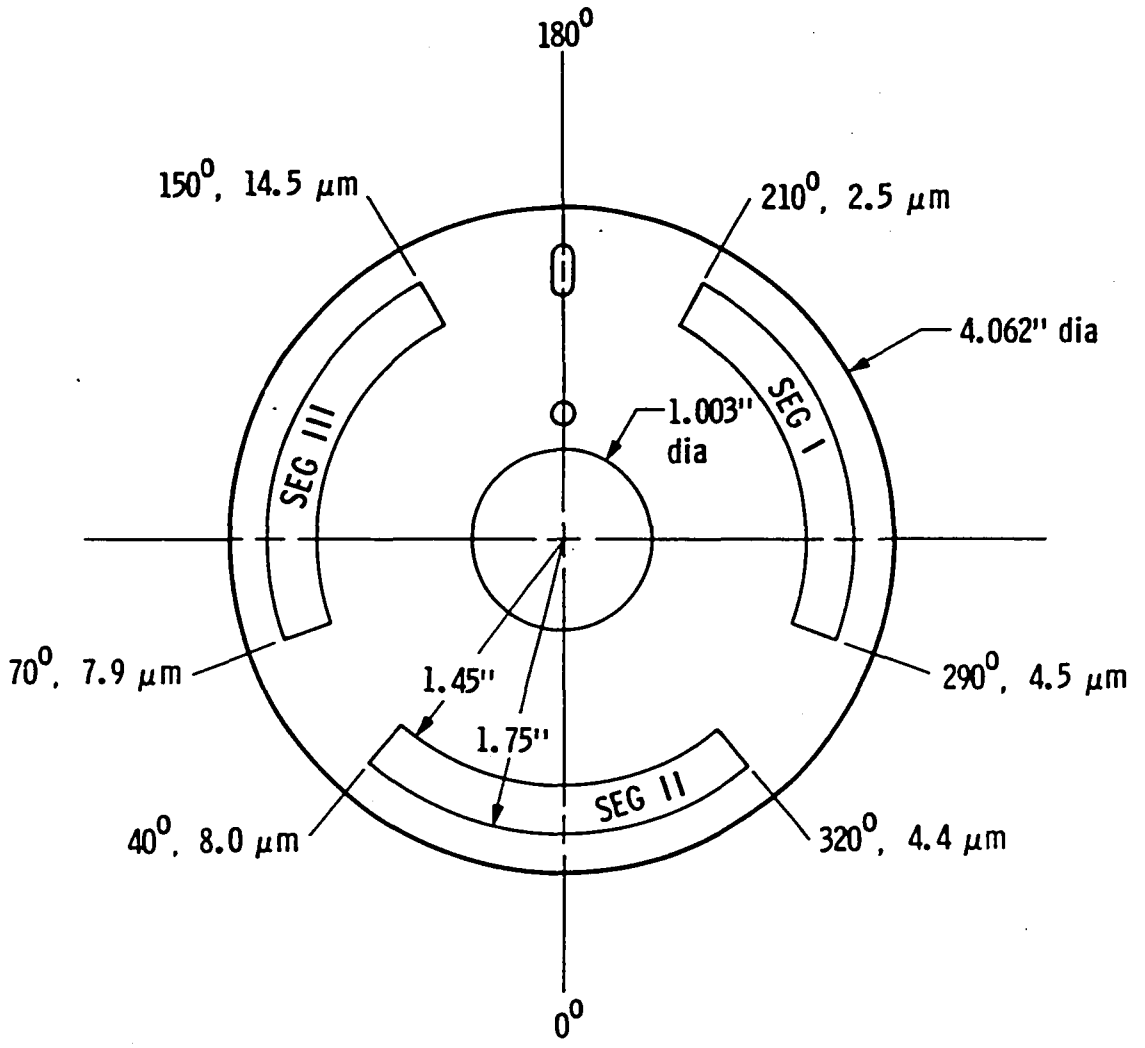

Figure 2-3. Filter Wheel

Table 2-2. Filter Wheel Specifications

(Optical Coating Laboratory, Inc., Model P/N W/2.5-14.4-1)

Segment 1	
Substrate:	Quartz, thickness: 0.015/0.020 in.
Blocking:	Less than 0.1% of average outside band, no peaks exceeding 0.5%
Half Bandwidth:	1.35% of wavelength
Range:	2.5 to 4.5 micrometers
Blocking Filter:	None
Transmittance	27%
Segment 2	
Substrate:	Germanium, thickness: 0.015/0.20 in.
Blocking:	Less than 0.1% of average outside band, no peaks exceeding 0.5%
Half Bandwidth:	1.35%
Range:	4.4 to 8.0 micrometers
Blocking Filter:	Irtran 1, thickness: 0.015/0.020 in.
Transmittance	32%
Segment 3	
Substrate:	Germanium, thickness: 0.015/0.020 in.
Blocking:	Less than 0.1% below pass band and above to 17 micrometers, no peaks exceeding 0.5%
Half Bandwidth:	1.8% of wavelength
Range:	7.9 to 14.5 micrometers
Blocking Filter:	Germanium, thickness: 0.015/0.020 in.
Transmittance	35%

2.3 CHOPPER MIRROR

A rotating chopper mirror, at an angle of 45 degrees to the optical axis, alternately passes radiation from the target and reflects radiation from an internal reference source. The chopping frequency is crystal controlled to a constant 488 Hz. An LED-photodiode edge detector, mounted at the edge of the chopper, provides a phase signal which is used for speed control and for synchronous demodulation of the spectral amplitude signal in the analog data processor.

2.4 INTERNAL REFERENCE

The internal reference consists of a disk of aluminum about 3.7 centimeters in diameter and 0.5 centimeter thick. It has a series of concentric, V-shaped grooves machined into its face and painted black. It is mounted on a massive heat sink, but no further provision is made for regulating its temperature. Reliance is placed on its thermal inertia to hold it at a steady temperature during a measurement. A thermistor is embedded in the disk to provide a temperature monitoring capability.

2.5 DETECTOR

The detector is a HgCdTe photoconductive junction device. Detector specifications are displayed in Table 2-3 and Figure 2-4. HgCdTe was chosen because of its extended range of spectral sensitivity and its superior detectivity. However, it requires cooling and its response is critically dependent on temperature. A small temperature sensor is mounted next to the detector inside the dewar to monitor the detector temperature. The output of the associated circuit is supplied to the data recorder. There is a safety interlock between the detector's temperature and its bias supply which protects the detector from being damaged by ohmic heating in its warm low impedance state.

Table 2-3. Detector Specifications

Material:	HgCdTe (photoconductive)	
Dimension:	1 x 3.5 mm	
Filter:	None	
Field of View:	Open	
Test Results:	Response (peak):	322 volt/watt
	N.E.P. (peak):	0.989×10^{-11} watt/$Hz^{1/2}$
	D* (peak):	0.189×10^{11} cm $Hz^{1/2}$/watt
	Resistance:	779 ohms
	Peak response:	11.6 microns
Test Conditions:	Frequency:	1000 Hz
	Band width:	50 Hz
	Detector temperature:	87.4 K
	B. B. flux density:	3.722 microwatts/cm^2
	B. B. temperature:	500 K
	Bias voltage:	1.5 volts
	Detector voltage:	1.2 volts
	Detector current:	1500 microamperes
	Feedback resistance:	221 ohms (load)
	Test gain:	10000

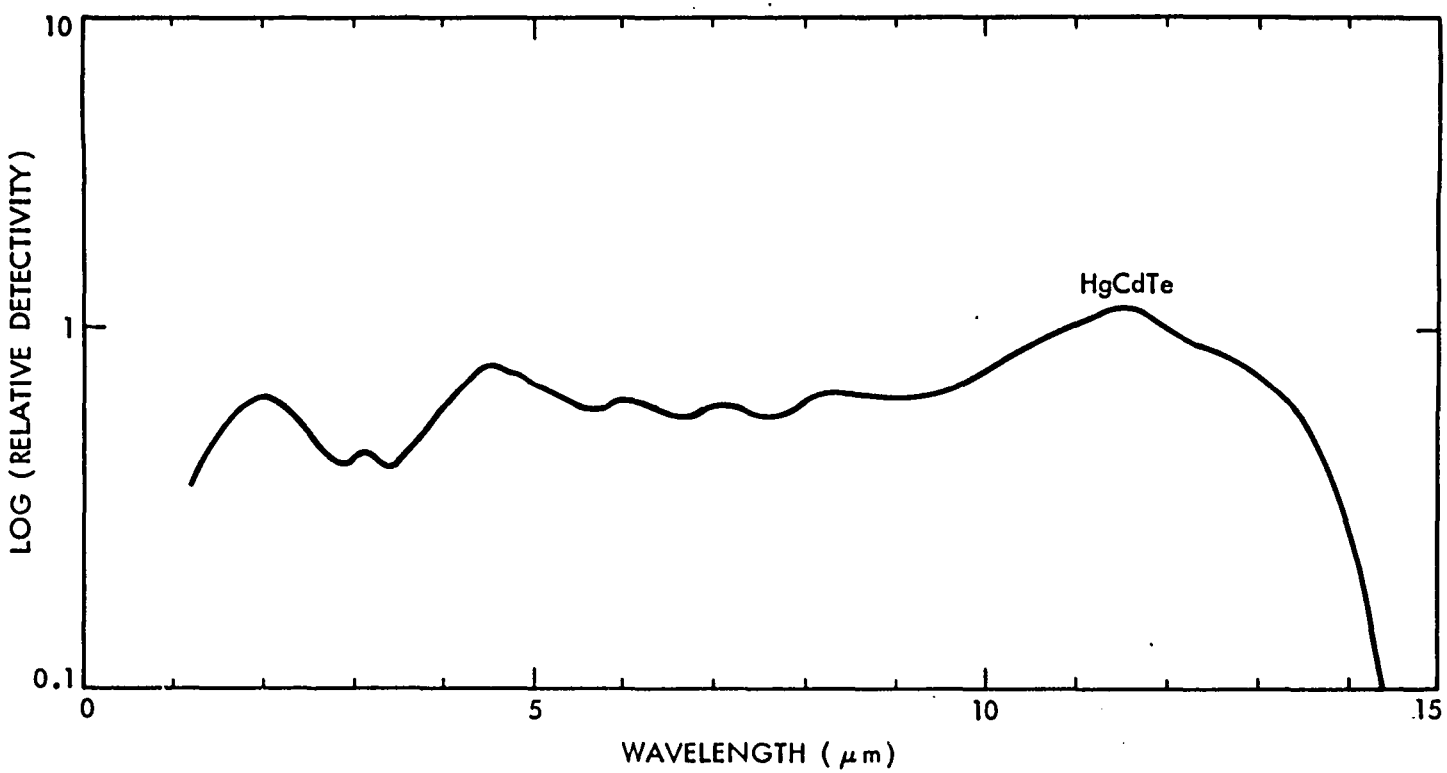

Figure 2-4. Log of Relative Detectivity of HgCdTe Detector

2.6 COOLING

The detector is mounted in a small dewar and is cooled by a Joule-Thompson cryostat. The cryostat consists of a helix of capillary tubing about 5 centimeters long and about 0.75 centimeter in diameter wound on a plastic form. High pressure argon gas from a supply tank is fed through the helix and jetted from a nozzle. The gas cools on expansion and flows back over the helix cooling the incoming gas. After a few seconds, low enough temperatures are reached to liquify part of the escaping argon. The liquid argon, a small amount of which accumulates in the cavity of the dewar, regulates the detector temperature to the boiling point of argon, which is 87.4 degrees Celsius at one atmosphere. The gas, which builds up in the sealed case, is vented to the outside through a low pressure relief valve.

We found that operating the cryostat at pressures above 1200 psi would result in temperature cycling which caused the detector response to vary by up to 7 percent. To prevent this, the high pressure argon gas is fed through a pressure regulator set at about 1000 psi, even though this unfortunately forfeits a substantial part of the cooling power of the argon. Before reaching the detector, the gas is made to flow through a molecular sieve drying filter to remove water vapor that would otherwise ice up the expansion nozzle.

The gas bottles we use hold 22 cubic feet of argon at the fully charged pressure of 2260 psi and weigh about 7 kg. One tank of gas is sufficient for a cool-down and about 45 minutes of operation.

2.7 PREAMPLIFIER

The preamplifier (see Figure 2-5 and Table 2-4) consists of a load resistor, bias circuit, and an ac coupled voltage mode amplifier appropriate for using the HgCdTe detector as a photoconductor. The circuit has an input impedance of 10k ohms and a gain of 80 dB. The bandwidth extends from 50 Hz to 350 kHz and the amplifier has a rise time of less than one microsecond. The bias current of the detector is adjusted to 1.5 milliamperes.

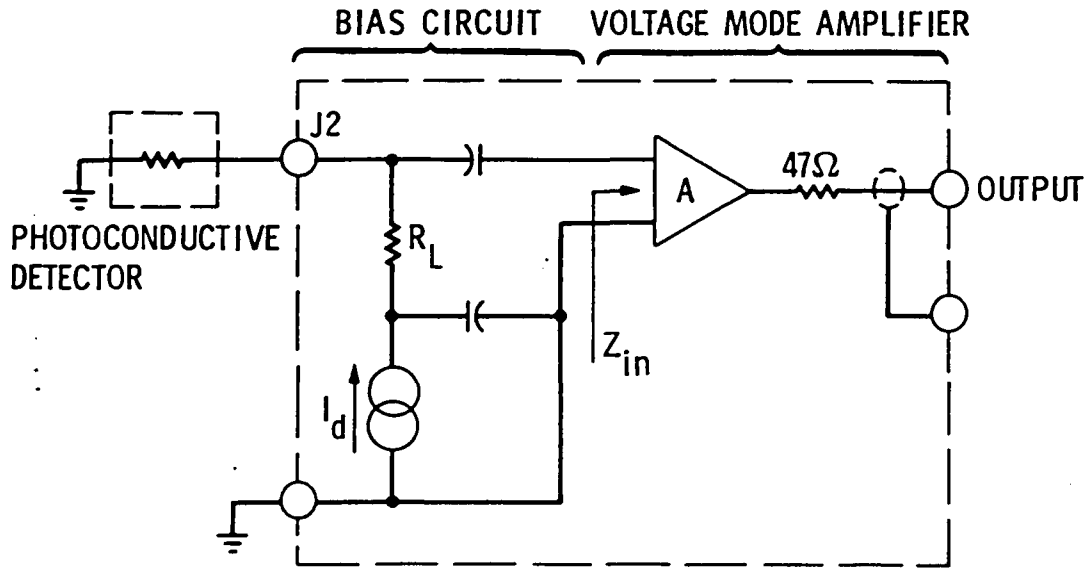

Figure 2-5. Preamplifier

Table 2-4. Preamplifier Specifications

Input Impedance:	Z_{in} = 10 k ohms
Output Impedance:	Z_o = 50 ohms
Voltage Gain:	A_v = 80 $\pm$ 1 dB (unterminated)
Maximum Output with	
10 k ohm load:	V_o = $\pm$10 volts peak
50 ohm load:	V_o = $\pm$0.5 volts peak
Load Resistor:	R_L = 301 ohms
Bandwidth	
Upper 3 dB frequency	$f_h \geq$ 350 kHz
Lower 3 dB frequency	$f_L \leq$ 50 Hz
Rise Time:	$t_r \leq$ 1 microsec
Shorted Input Noise:	$\bar{V}_n \leq$ 1.3 nV/Hz$^{1/2}$ at 10 kHz
Dc Output Voltage:	$V_{dc} \leq$ -34 mV
Detector Bias:	I_d = 1.5 mA (internal)
Power Requirements:	+15 Vdc at 23 mA
	-15 Vdc at 41 mA

2.8 POST-AMPLIFIERS

Upon leaving the preamplifier, the signal is routed to one or the other of two single stage level adjusting amplifiers depending on which filter segment is currently being scanned. An electronic filter is placed after these amplifiers which passes a band centered on the 488 Hz chopping frequency. The output of this filter, which is a nearly monochromatic sine wave, is sent to the data recorder for further processing, conversion, and recording.

SECTION 3

DATA RECORDER

The data recorder prepares the analog data for conversion, converts it to digital form, assembles a data word for each sample point, and records the data words onto digital tape. The pack frame mounted box which houses the data recorder also contains the operator controls and the power supply. The data recorder functions are described separately below and in Figure 3-1.

3.1 ANALOG PROCESSING

The analog processor (Figure 3-2) receives the ac data signal from the sensor head and prepares it for digital conversion. The steps include amplification, demodulation (rectification), integration, sampling the signal, and holding it for conversion to digital form.

The processing begins with a stage of gain. Proper gain selection is made by the operator who monitors the output of the analog processing section with a meter. Eight different levels are available covering gains proportional to 1, 2, 5, 10, 20, 50, 100, and 200.

After amplification, the ac signal is rectified using analog FET switches controlled by a signal derived from the chopper phase. Appropriate phase delay is introduced using a crystal controlled timer.

The rectified signal is accumulated on an integrating capacitor for a period of time derived by counting an integral number of chopper cycles. At the end of the integration period, the voltage on the integration capacitor is sampled by a holding circuit which maintains it during analog to digital conversion. Subsequent to sampling, the integrating capacitor is discharged (dumped) to ground.

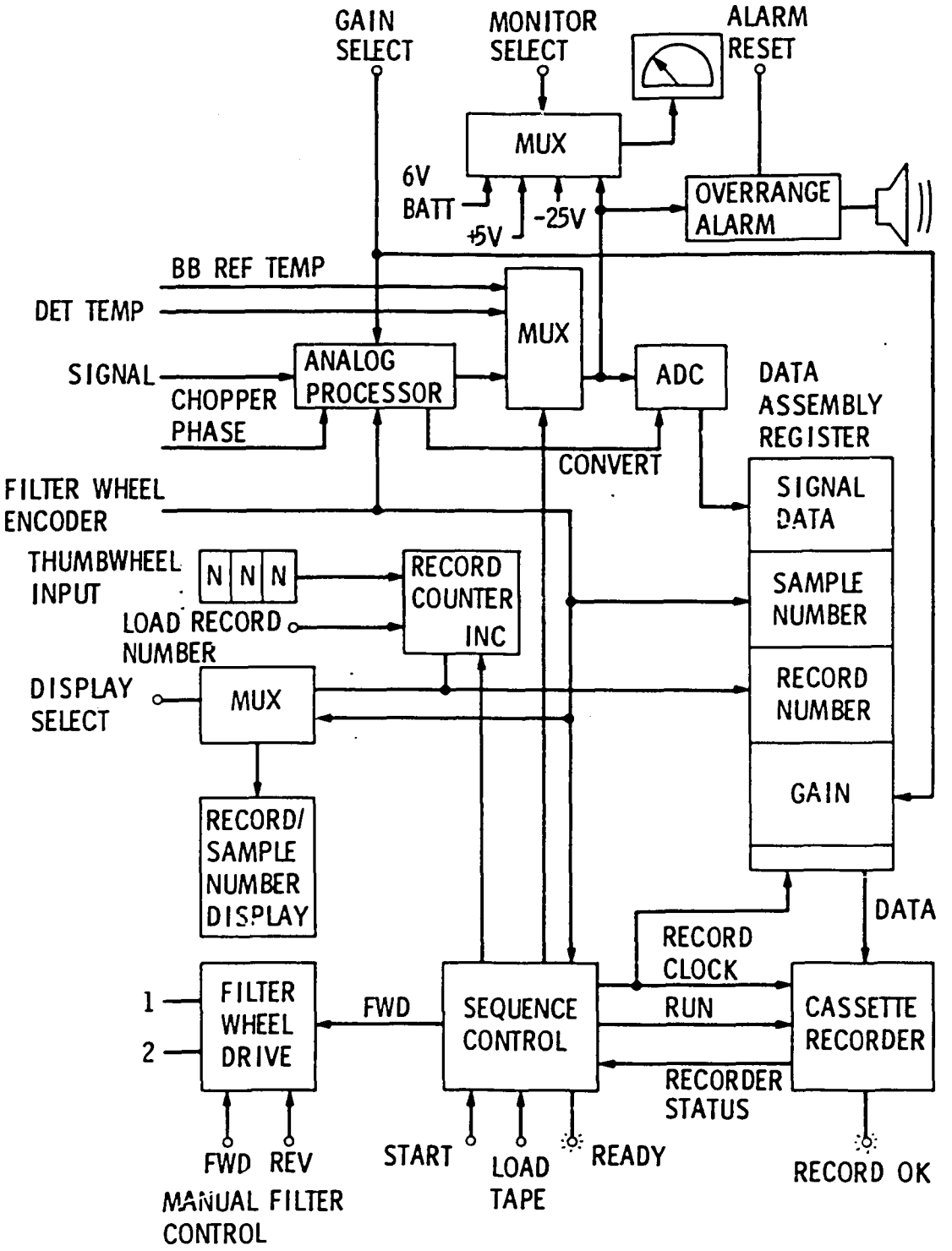

Figure 3-1. Functional Diagram of Data Recorder

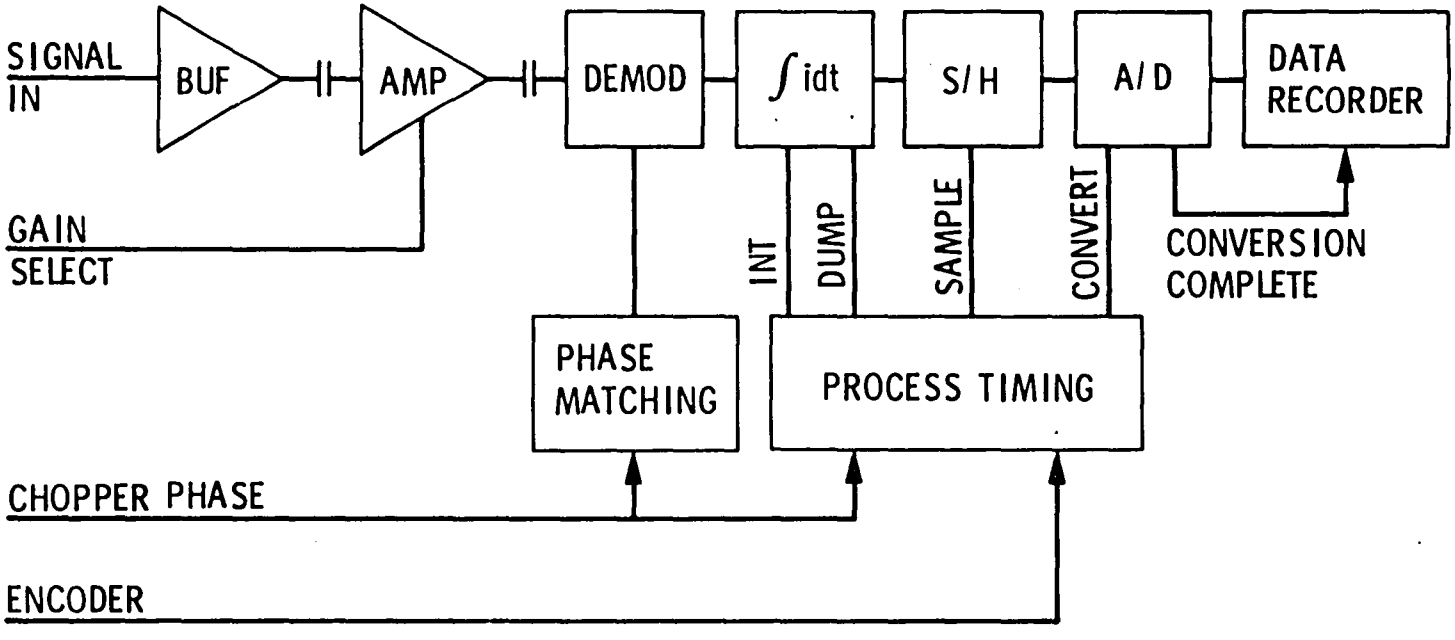

Figure 3-2. Organization of Signal Processor

The timing signals that control the beginning and end of the integration cycle, the dumping of the accumulated charge, the sampling, and the start of conversion are all derived with suitable delays from the transitions of the filter wheel encoder.

A data selector operating under control of the filter wheel encoder selects the signal to be converted from three different sources, the analog processor, the detector temperature measuring circuit, and the internal reference temperature monitor. In this way, information vital to the interpretation of the data can be interspersed with the spectral data during the time it takes for the filter wheel to scan between the filter segments.

3.2 CONVERSION

Analog to digital conversion of the signal is carried out by a 12 bit successive approximation converter with a conversion time of 40 microseconds. Only the ten most significant bits are recorded.

3.3 RECORD COUNTER

An eight-bit record counter which is automatically incremented at the beginning of each tape record provides a control panel display of the record number and a digital input to the data word for each sample. It can be preset by a thumbwheel and reset button.

3.4 DATA WORD ASSEMBLY

A data word of 48 bits is assembled into a parallel in/serial out shift register. The 48 bits include eight bits from the record counter, ten bits of spectral data, nine bits from the filter wheel encoder, three bits to specify the gain, and various other bits required by the format and parity checking. Provision was made for an extra ten-bit field within the data word for recording another channel of spectral data, but it is not being used.

When the output of the converter has stabilized, the converter sends a conversion complete signal which initiates the read out of data to the recorder.

3.5 RECORDING

The digital tape recorder records 50 complete spectra on each side of a standard Phillips tape cassette. The starting and stopping of the capstan motor are made to occur at the appropriate time in the recording cycle by digital logic which reads the codes produced by the filter wheel encoder. The tape speed is slightly below 5 centimeters per second. The bit transfer rate of 1200 bits per second is fast enough to allow for gaps between successive data words despite some unevenness in the time intervals between successive encoder transitions.

3.6 POWER SUPPLY

The primary power source is a silver zinc battery weighing 4.3 kg (9-1/2 lb) and rated at 80 ampere hours. Fully charged its voltage is about 7.4 volts which declines to about 6 volts on its long and gradual discharge plateau. To power the electronics, custom converters were built which provide regulated voltages of plus and minus 15 and plus 5. Standard converters and regulators are used to provide the other voltages required, except for one case which is satisfied by a 2.5 volt lithium cell. One charging of the main battery is sufficient for about 3 hours of continuous operation. Figure 3-3 outlines the power system.

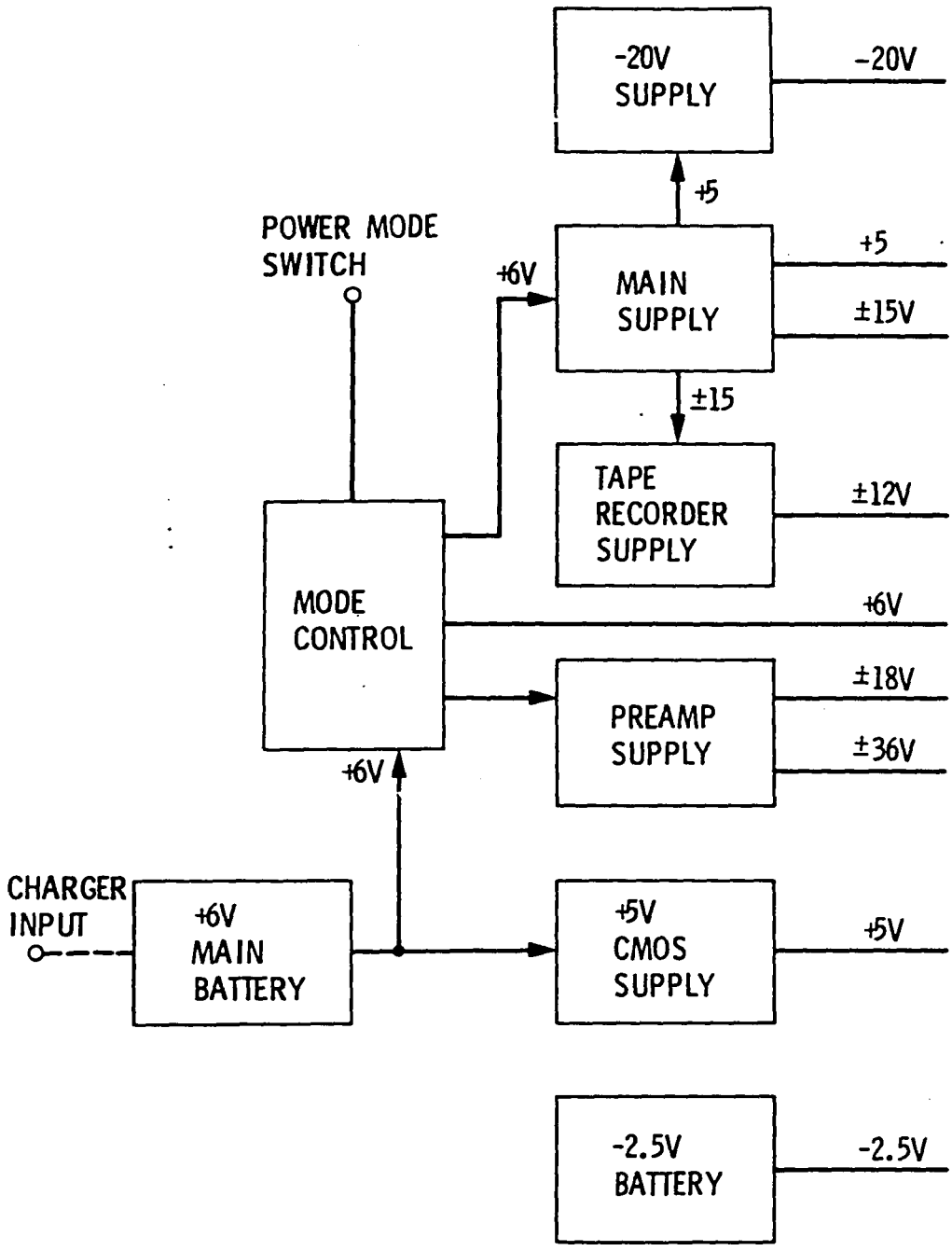

Figure 3-3. Power System

SECTION 4

OPERATING CONTROLS

The operating controls are concentrated on a small panel on the data recorder box and on a monitor head which is connected to the main box by a four foot cable. The control layout can be seen in Figure 4-1. Table 4-1 describes the function of each switch, pushbutton, and light.

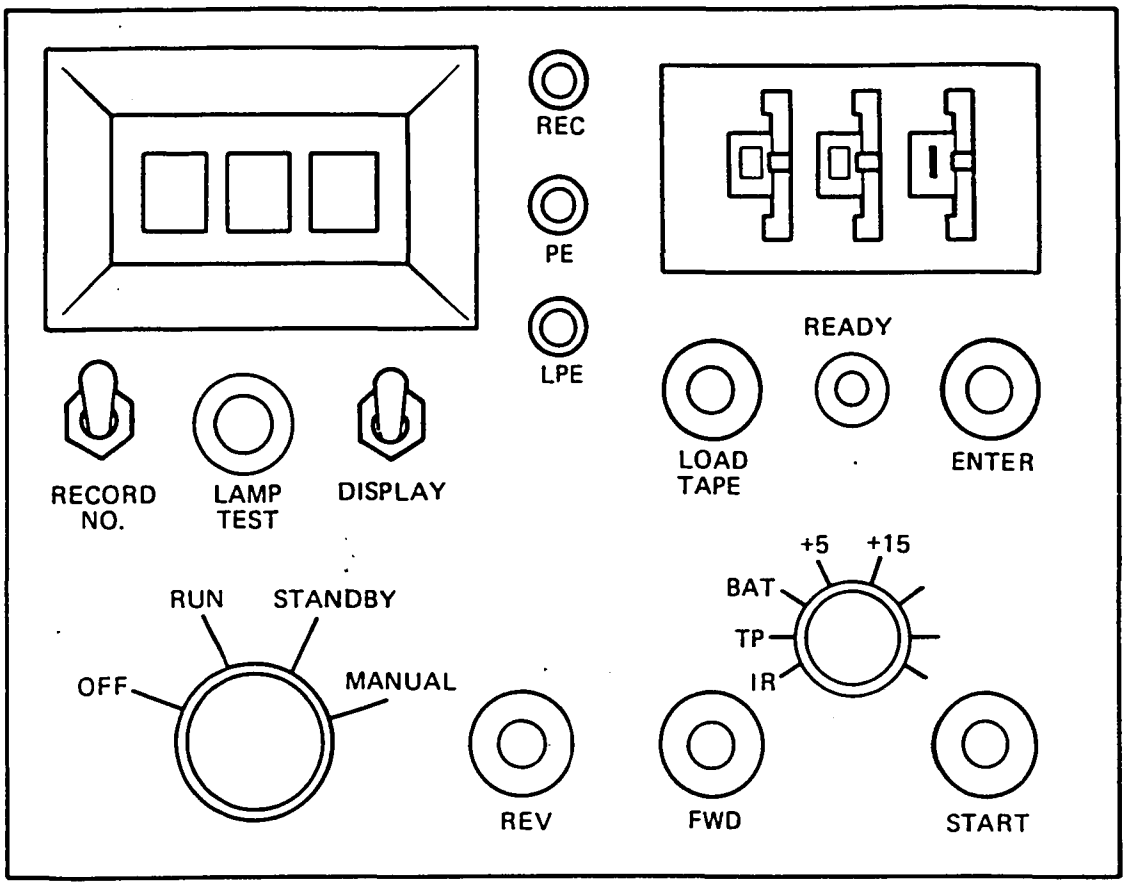

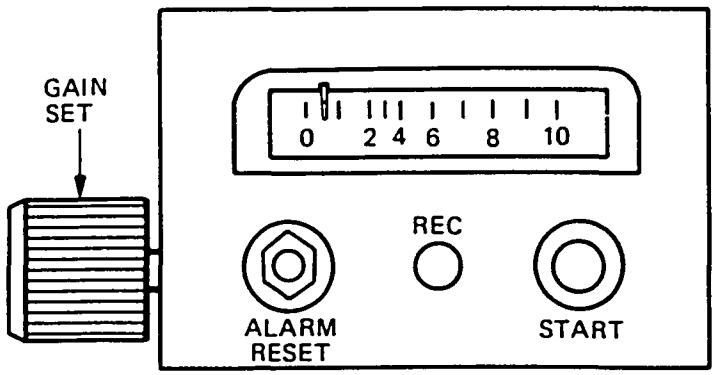

Figure 4-1. Operating Controls and Displays

Table 4-1. Front Panel Functions and Displays

LOAD TAPE	Starts tape loading sequence
LAMP TEST	Turns on all segments in LED panel
ENTER	Resets record number to value set on thumbwheel switch
REV	Drives filter wheel in reverse
FWD	Drives filter wheel forward
START	Starts scanning and recording of a spectrum
RECORD NO.	Selects whether LED panel will display record number of sample number
DISPLAY	On/off switch for LED panel
OFF.....MANUAL	Selects power status
IR, TP, BAT, etc	Selects which signal goes to meter in monitor head
REC	Flashes on and off to indicate proper recording
PE and LPE	Flash when error condition is detected in record
READY	Lights up when ready to scan next spectrum
MONITOR HEAD:	
GAIN SET	Rotary switch selects among 8 gain levels
START	Same as START on front panel
REC	Same as REC on front panel
ALARM RESET	Squelches overrange alarm

SECTION 5

FIELD PROCEDURES

While in the laboratory, the head is usually supported on a stationary frame. For field use, however, one member of the operating team stands with the sensor pack frame on his back aimed at the target. For targets where this might be too awkward, the pack is taken off and some alternative support is improvised. The other member of the team selects the proper amplifier gain, watches the signal level monitor and the lights that indicate proper recording. A third member may be employed in collecting samples and keeping a written log of site description, instrument settings, time of day, and other particulars.

All spectral measurements are made relative to the spectrum of a reference blackbody which is taken along into the field for the purpose. This blackbody is a sheet metal horn made of aluminum and painted black inside and out. See Figure 5-1. It is covered with a 2.5-centimeter layer of insulating foam, except for its 8.75-centimeter square mouth. The foam helps to insure temperature stability. A thermistor has been glued to the metal wall of the horn to measure its temperature.

Usually about four spectra of each target are measured to provide a check of consistency and to reduce noise by averaging. The same number of reference spectra are made using the reference blackbody. The temperature of the reference must be measured and logged each time. Each spectrum takes about 30 seconds to scan; a complete set of four target spectra and four reference spectra can be completed in about five minutes.

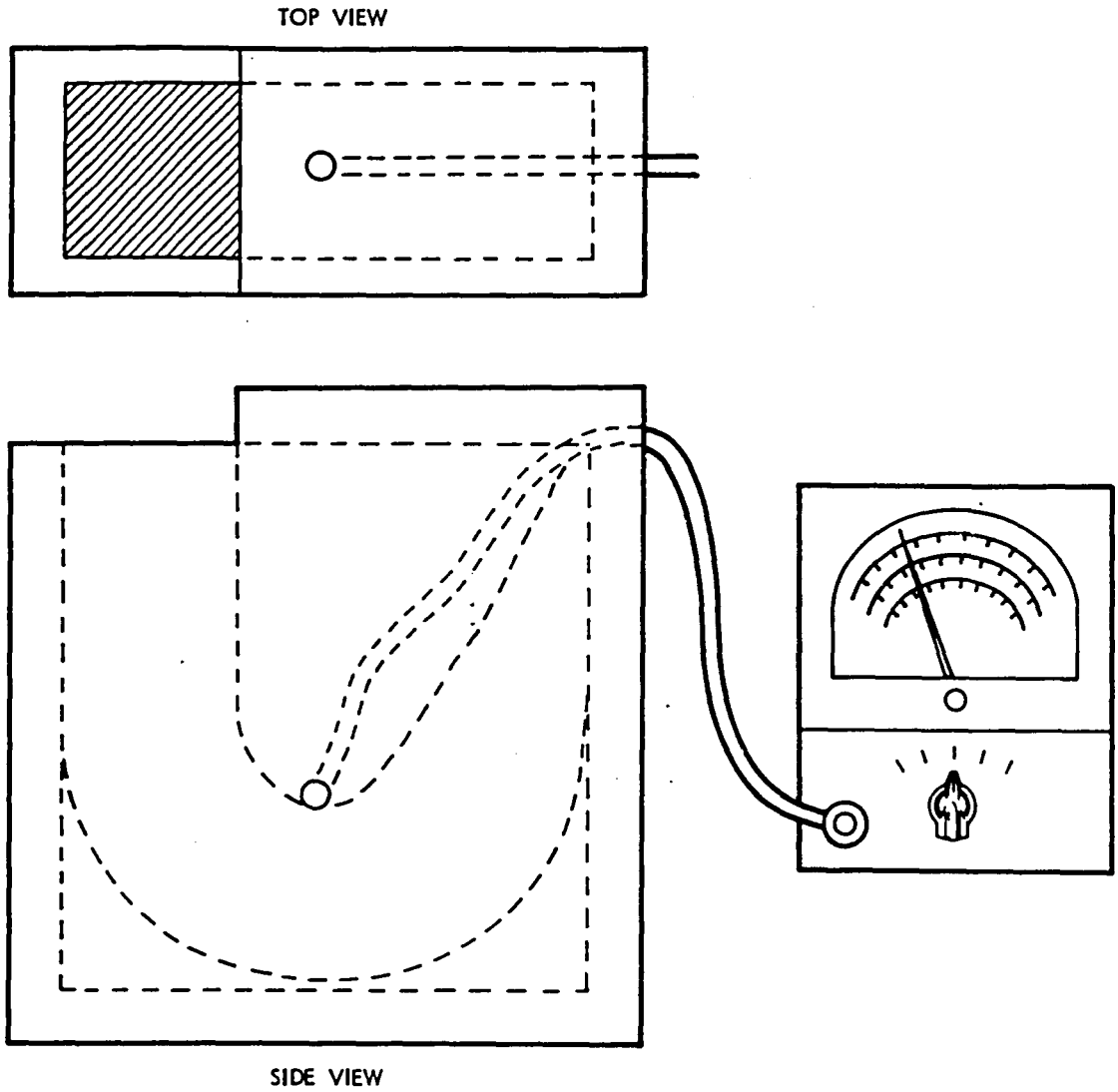

Figure 5-1. Reference Blackbody Horn

SECTION 6

TREATMENT OF DATA

The following discussion uses a simplified model of the spectrometer which is adequate to explain the most important aspects of its behavior.

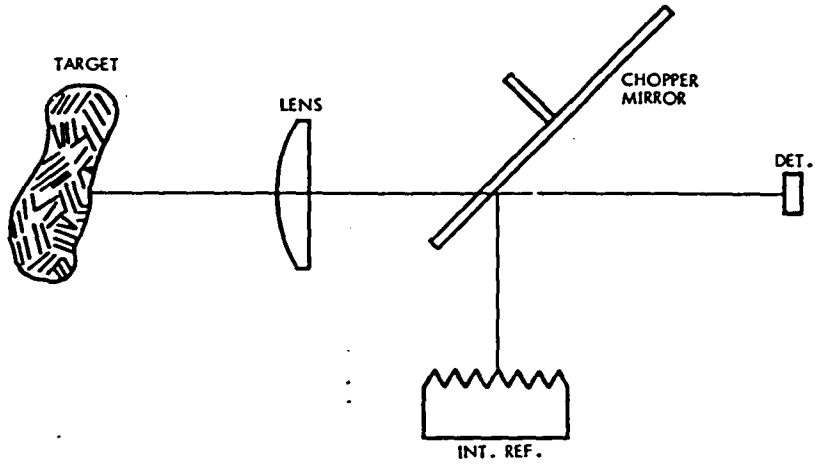

Figure 6-1. PFES Conceptual Model

The detector produces an ac signal of amplitude proportional to the difference between the radiance from the target and the radiance from the internal reference, which are alternately selected by the chopper. The ac signal is rectified and converted to digital form for recording on tape. The digital output, N , is related to the input by the following equation.

$$(1)\ N_{TARG} = K\ (R_T\ L - R_{REF}\ M + R_L - R_M)$$

Where:

N_{TARG} = Digital response
R_L = Radiance of lens
R_M = Radiance of mirror
R_T = Radiance of target

R_{REF} = Radiance of internal reference
M = Reflectivity of mirror
L = Transmission of lens
K = Responsivity of the detector

The transmission of the lens and the reflectivity of the mirror are assumed to be constant over the temperature range encountered in practice.

Applying this relationship to measurements of the target and an external reference blackbody, we get:

$$(2)\ N_{TARG} = K(R_T\ L - R_{REF}\ M + R_L - R_M)$$

$$(3)\ N_{BB} = K(R_{BB}\ L - R_{REF}\ M + R_L - R_M)$$

Provided the two measurements are made close together in time, the thermal inertia of the lens, chopper, and internal reference will allow us to assume that their contributions are essentially constant. Taking the difference between (2) and (3) we get

$$(4)\ N_{TARG} - N_{BB} = KL(R_T - R_{BB})$$

which can be inverted to give R_T, the radiance of the target.

$$(5)\ R_T = R_{BB} + (N_T - N_{BB})/KL$$

In this equation R_{BB} is calculated from the Planck formula and the KL divisor is drawn from a table which has been generated from measurements made on blackbodies of different temperatures. For example, applying Equation 5 to blackbodies BB1 and BB2 and solving for KL, we get

$$(6)\ KL = (N_{BB1} - N_{BB2})/(R_{BB1} - R_{BB2}),$$

where R_{BB1} and R_{BB2} are calculated and N_{BB1} and N_{BB2} are the digital responses. When the digital responses at a given wavelength are plotted versus the temperatures of the blackbody for various temperatures, the points lie very close to a line of slope KL. The slope of the line which fits the points best from the point of view of minimizing the sum of the squares of the deviations in digital response is accepted as the responsivity of the instrument for the wavelength in question.

Deriving the KL divisors constitutes the response calibration of the instrument. Blackbody temperatures are used ranging from 0 to 55 degrees Celsius.

Some examples of raw data taken during calibration are contained in Figure 6-2. The four curves were made using the blackbody horn described above. From top to bottom, they correspond to 36.7 degrees Celsius at gain 5; 36.6 degrees Celsius at gain 4; 11.1 degrees Celsius at gain 4; and 10.9 degrees Celsius at gain 5.

For the identification and comparison of materials the emissivity is required rather than the radiance since the emissivity is a property of the material which is independent of environmental effects. Over the limited range of temperatures encountered in the field the temperature variations of emissivity can be ignored.

(In using the term "emissivity" in a slightly more general sense, namely where the conditions of equilibrium are not strictly satisfied, we may be further polluting the already murky waters of photo-terminology. Nevertheless, the authors have deliberately chosen to use "emissivity" rather than some other term such as "emittance" because they believe "emissivity" more effectively conveys the idea to a general audience.)

Emissivity is derived by dividing the radiance of the material by the radiance of a blackbody at the same temperature. There is a further provison, however, that the material must be in radiative equilibrium with its surroundings. If not, temperature gradients manifest themselves in the outer

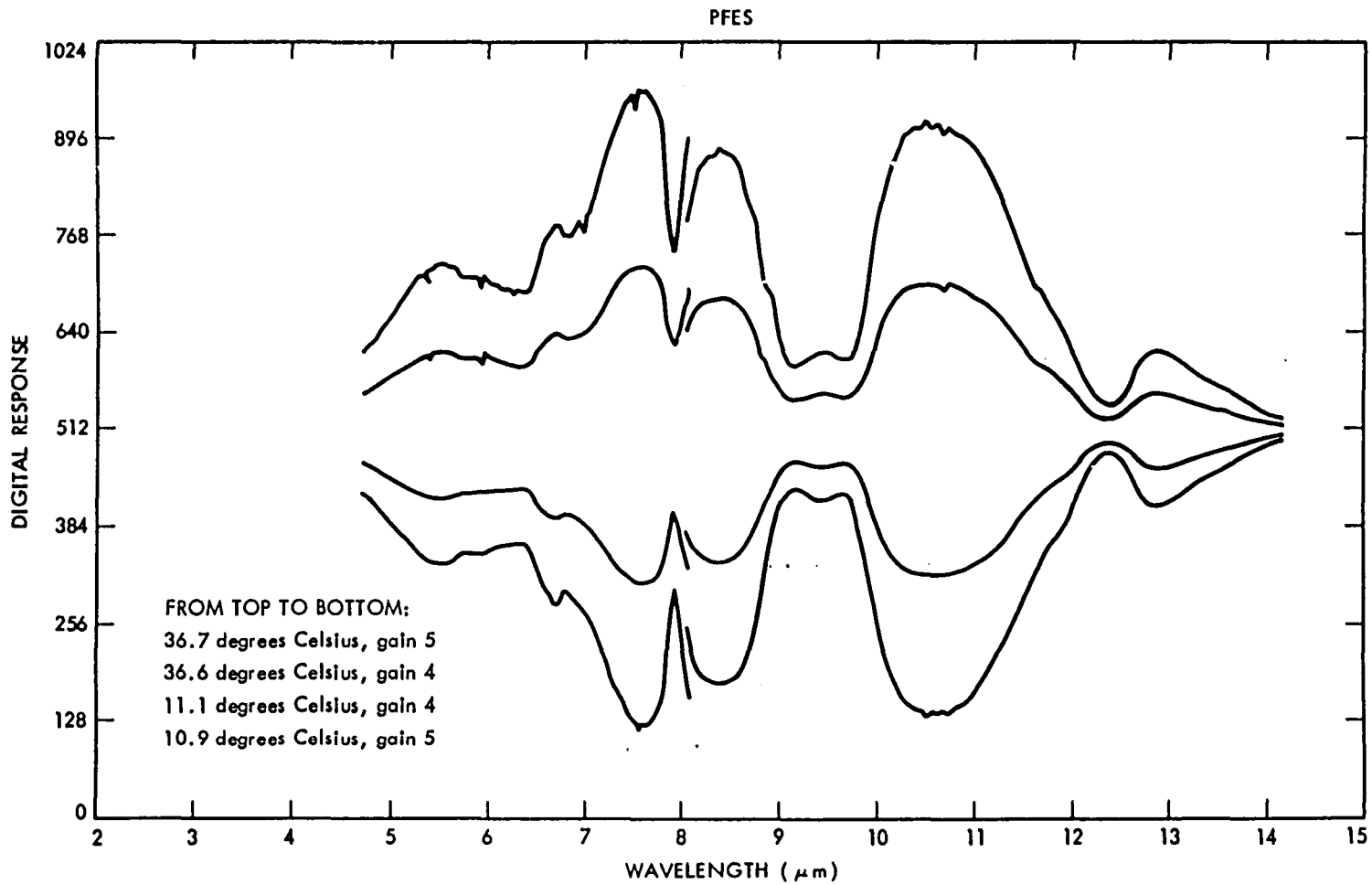

Figure 6-2. Raw Spectral Data

radiating skin of the material, possibly distorting the result. The conditions encountered in practice most often violate the equilibrium requirement to some extent, but, as a practical matter, the deviation is usually of negligible importance. It is difficult to measure or estimate the effective radiating temperature of the materials, because of their inhomogeneities. Also significant are variations across the target surface that arise from shadowing or possible variations in thermal diffusivity.

In cases where the material is not in radiative equilibrium with its surroundings, the effective radiating temperature of the surface will not be the same as that measured by contacting the surface with a probe. However, at certain frequencies, in the regions of anomalous dispersion, all materials will emit with an efficiency close to that of a blackbody. The emission spectrum can be fitted to a calculated blackbody spectrum by adjusting the temperature of the calculated blackbody spectrum until it matches the sample spectrum at the frequencies of anomalous dispersion. The ratio of the sample spectrum to the fitted blackbody spectrum then gives an estimate of the emissivity under the assumption that the sample behaves like a blackbody at the selected frequencies. This method was exploited by Conel (Reference 6-1, 1969) to determine the emissive properties of silicates in the laboratory. Refer to that paper for details.

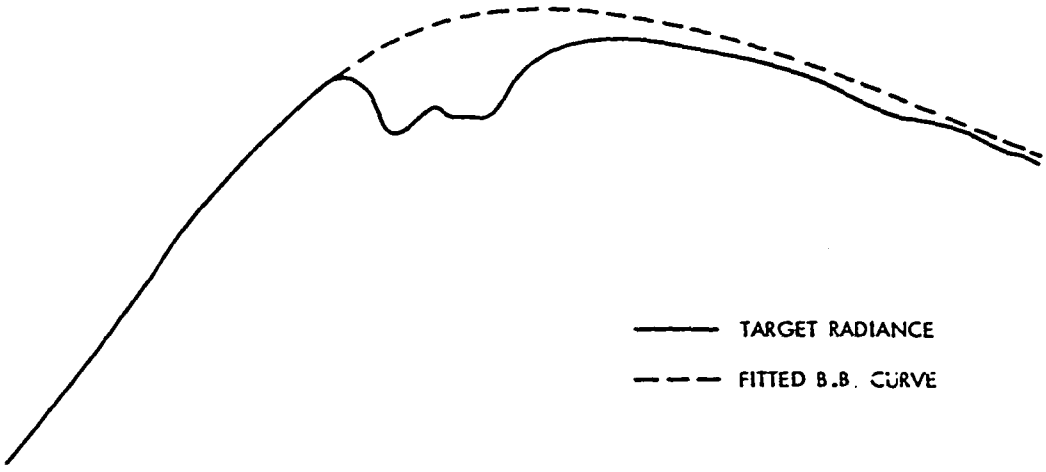

Figure 6-3. Fitting Blackbody Curve to Target Radiance

Most materials encountered in our work are not pure, but consist of mixtures. Nevertheless, the above method constitutes the best available working approximation. The extent of the limitation is not known to us at the present time, and must await absolute measurements of reflectance for selected targets. However, for most of the materials we have examined, it is possible to fit blackbody curves over substantial portions of their spectra. Therefore, we feel justified in continuing to treat mixtures and pure substances in the same manner with regard to determining their emissivities and their effective radiating temperatures.

SECTION 7

SYSTEM PERFORMANCE

7.1 SPECTRAL RESOLUTION

The spectral resolution of the instrument is largely determined by the filters in the analyzer. According to the manufacturer, the resolution of the 4.5 to 8.0 micrometer segment is 1.5 percent and that of the 7.9 to 14.5 micrometer segment, 1.8 percent. The resolution curve displayed in Figure 7-1 is based on the manufacturer supplied information with allowance made for the effective slit width.

In order to check the total system resolution, scans were made of CO_2 laser light scattered from a diffusing surface of gold coated 600 grit sandpaper. The spectral line selected was that at 10.588 micrometers. The line profile produced is shown in Figure 7-2. It can be determined from the response profile that the resolution is limited to a spectral extent of about three samples at the wavelength of the laser. This is equivalent to 1.5 percent.

An indication of the performance with a complicated spectrum containing many narrow features can be obtained by examining Figure 7-3 which was produced by looking at a blackbody continuum through a thin absorbing layer of polystyrene. The lower curve is from the PFES while the upper one was made on a laboratory Fourier transform spectrometer (Analect model 6200). The resolution of the Analect is approximately four wavenumbers which equates to 0.25 percent at 10 micrometers.

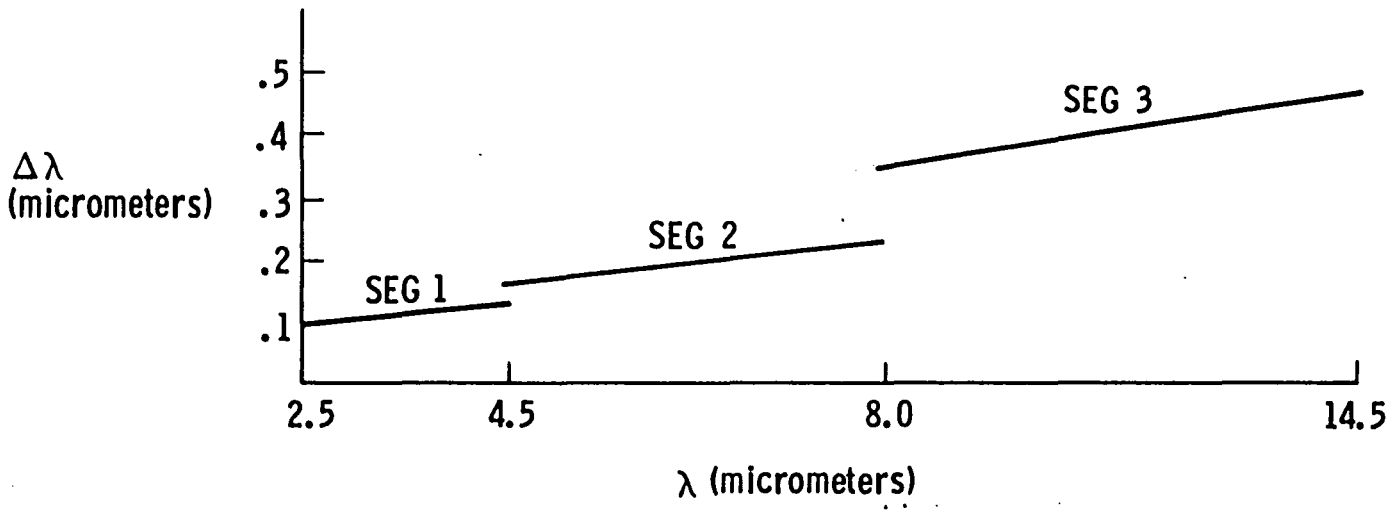

Figure 7-1. Spectral Resolution (Calculated from Optical Specifications)

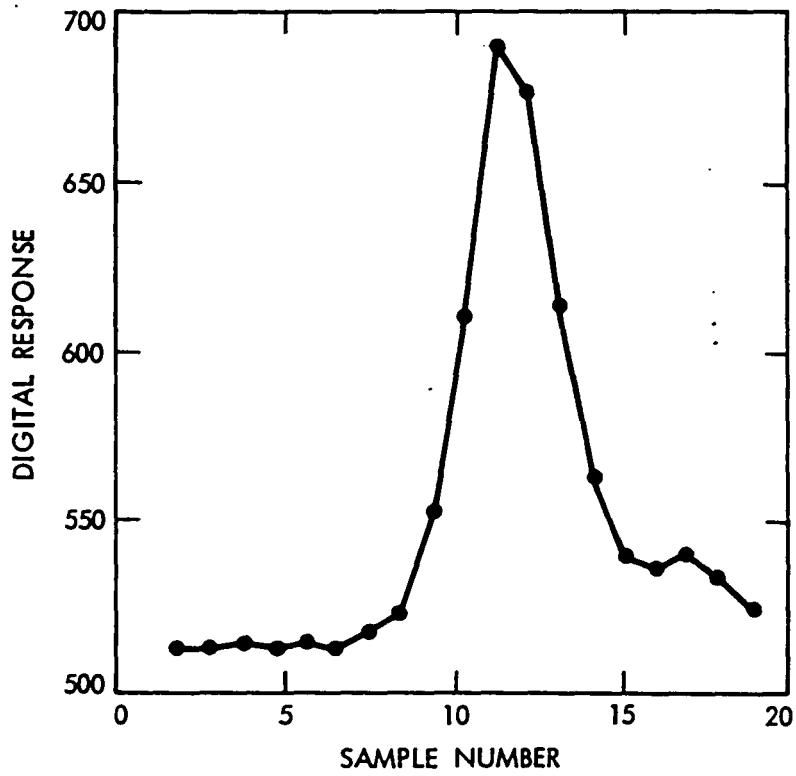

Figure 7-2. Response Profile to CO_2 Laser Line at 10.588 Micrometers

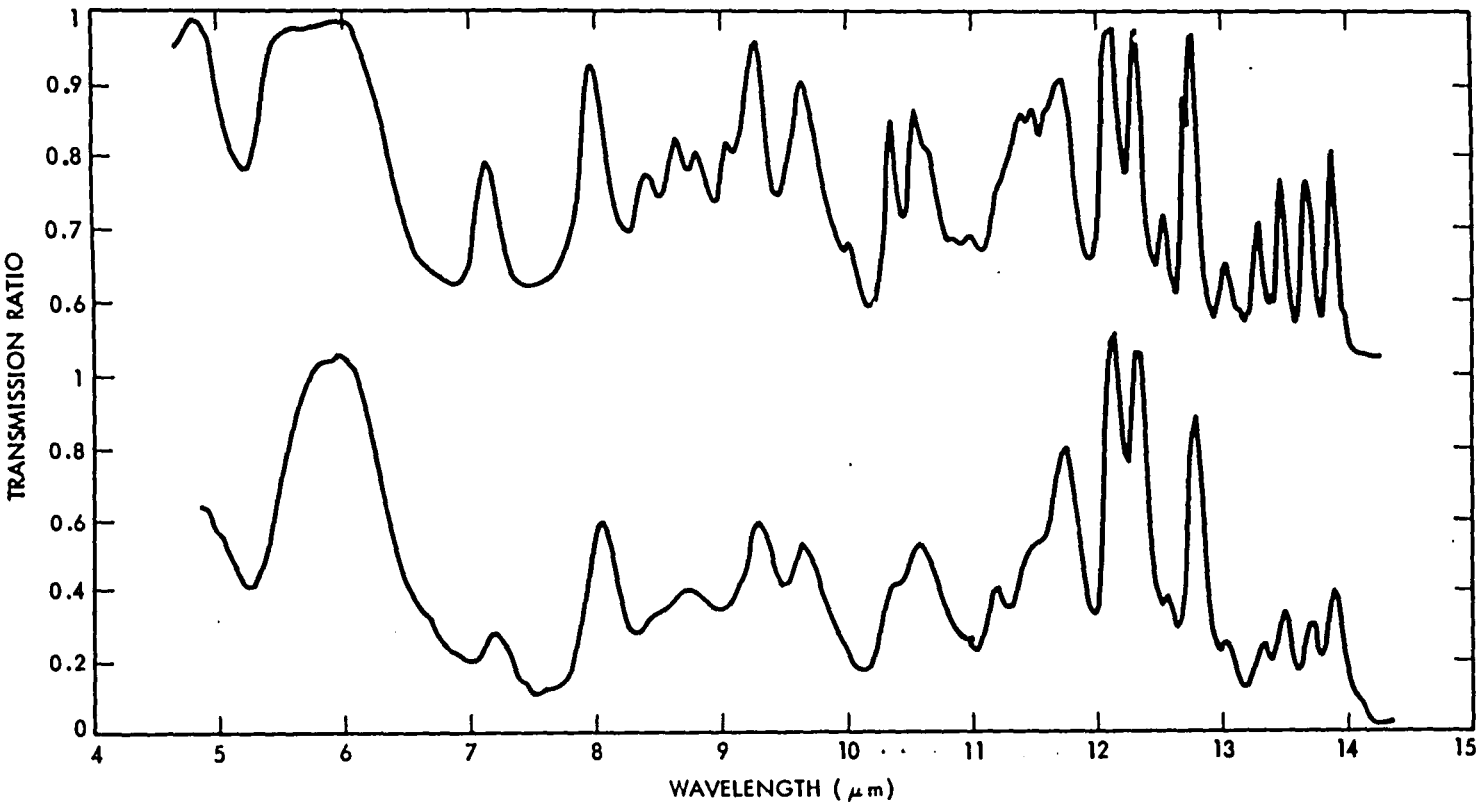

Figure 7-3. Comparison of Polystyrene Transmission Spectra
(Top: Analect 6200 Bottom: PFES.)

7.2 RADIANCE RESOLUTION

To determine the radiance resolution of the total system, a number of spectra were made, using a laboratory blackbody maintained at a constant temperature approximating that of the spectrometer, 24 degrees Celsius. Using the spectra by pairs one can calculate radiances for the ambient black body. The standard deviation of the set of spectra then gives a fair measure of the minimum detectable radiance for one spectrum. Twenty-three consecutive pairs were considered. Multiplying the standard deviation of the radiance measurements by Δtemperature/Δradiance for a 24 degree Celsius blackbody gives the noise equivalent ΔT, ($NE\Delta T$), and ratioing the standard deviation of the radiance to the calculated radiance for the blackbody produces the signal to noise ratio. Plots of the standard deviation of the radiance, the $NE\Delta T$, and the signal to noise ratio are contained in Figure 7-4.

7.3 ABSOLUTE SPECTRAL CALIBRATION

For the purpose of absolute spectral calibration, reference was made to the accepted values for the absorption peaks in the polystyrene spectrum already referred to. The maximum error anywhere observable was one half of a sample. This corresponds to one sixth of a spectral resolution element. To date, we have no reason to suspect the stability of the wavelength calibration either from deterioration of the filters or from slippage between the filter wheel and the angle encoder.

7.4 ABSOLUTE RADIANCE CALIBRATION

Absolute errors in radiance come primarily from two sources, changing responsivity of the detection system and errors in measuring the temperature of the reference blackbody.

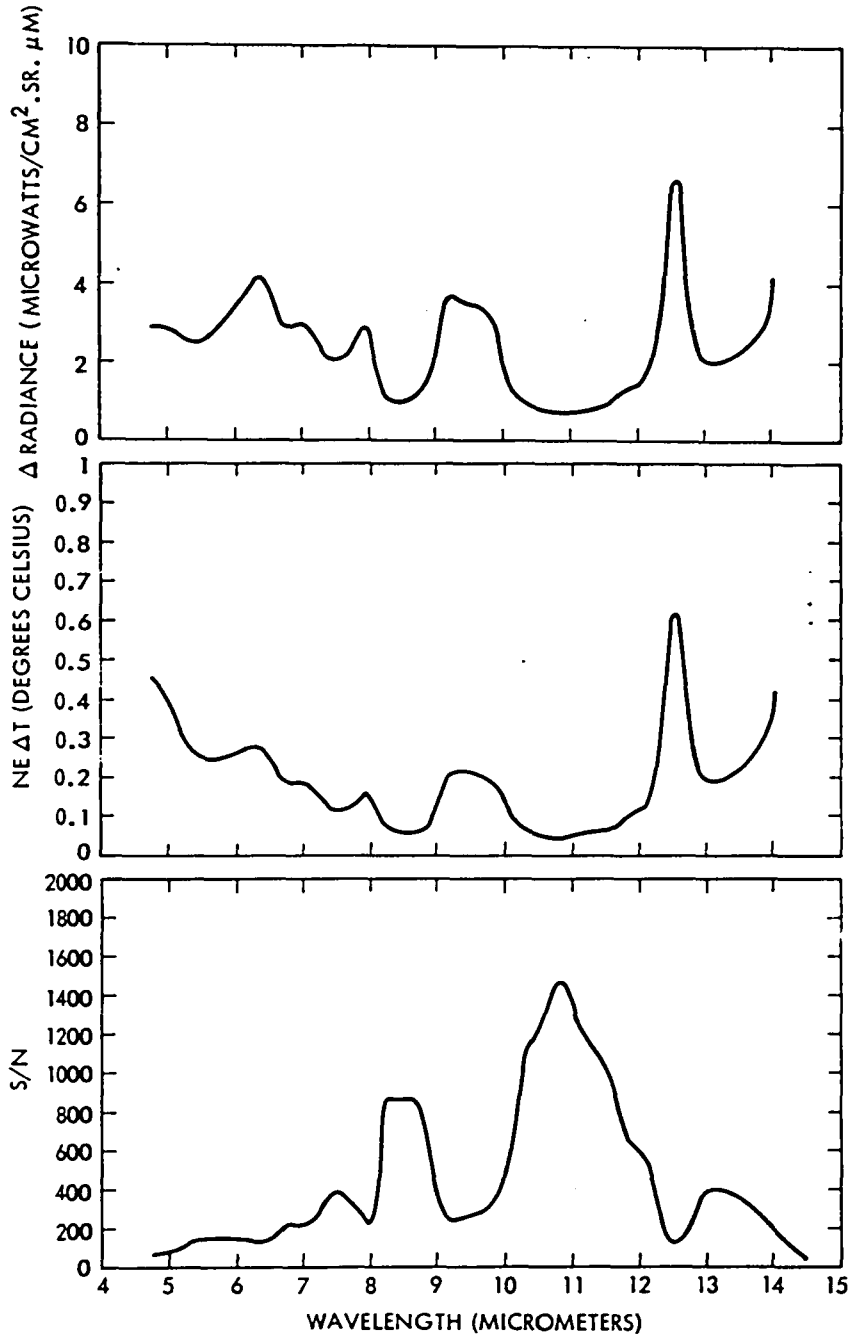

Figure 7-4. Top: Standard Deviation of Radiance
Middle: NEΔT
Bottom: Signal-to-Noise Ratio
All Refer to Measurements of a Blackbody at
24 Degrees Celsius

The temperature of the reference blackbody is measured using a thermistor and a commercial meter, the YSI Model 42SC. Temperature readings from the thermistor coincided with those from a mercury thermometer to within 0.2 degree Celsius when both were immersed in a stirred water bath at various temperatures ranging from 0 to 55 degrees Celsius. Measurements made simultaneously at different points on the reference horn indicated that isothermality can be maintained to within 0.5 degree Celsius if care is taken not to expose the horn to direct sunshine or the warmth of the operator's hands. A smooth variation of 0.5 degree Celsius from point to point within the horn could give rise to an error in measured radiance as great as 0.8 percent at 4.5 micrometers or 0.3 percent at 14 micrometers.

Variation in the responsivity of the detection system can be caused by aging of the optical and electronic components. So far, the system appears reasonably stable over a time span of a few weeks. Periodic recalibration using the method outlined in the discussion of data handling earlier in this paper seems advisable. We should point out, however, that any errors arising from changes in responsivity are going to be proportional to the difference between the radiance of the target and the external reference. The fact that target and reference both follow roughly the temperature of the environment mitigates the problem.

SECTION 8

EXAMPLES

Reduction and plotting are currently carried out on a VAX 750 and a Hewlett Packard pen plotter. The program enables the user to select from a menu of different forms of display which include raw data, radiance, calculated and fitted blackbody curves, and emittance. Averages and standard deviations are also available.

Figures 8-1 through 8-4 are examples of what has become our standard output. Each sheet contains plots of radiance, a blackbody curve fitted to the radiance, and the emissivity ratio. Each of these spectra are of naturally occuring materials identified in situ by inspection. They should not be considered as spectra of pure samples.

These spectra were chosen as typical of the hundreds we have measured. The gypsum-bearing soil, quartzite, and dolomite all show the spectral features we would expect for these materials based on published laboratory measurements [Lyon, 1964 (Reference 8-1); Hunt and Salisbury, 1976 (Reference 8-2); Hunt, 1980 (Reference 8-3)] and our own laboratory reflectance measurements using the Analect 6200. The spectrum of the desert holly plant is typical of all the spectra of desert plants that we have measured, resembling a black (or possibly gray) body.

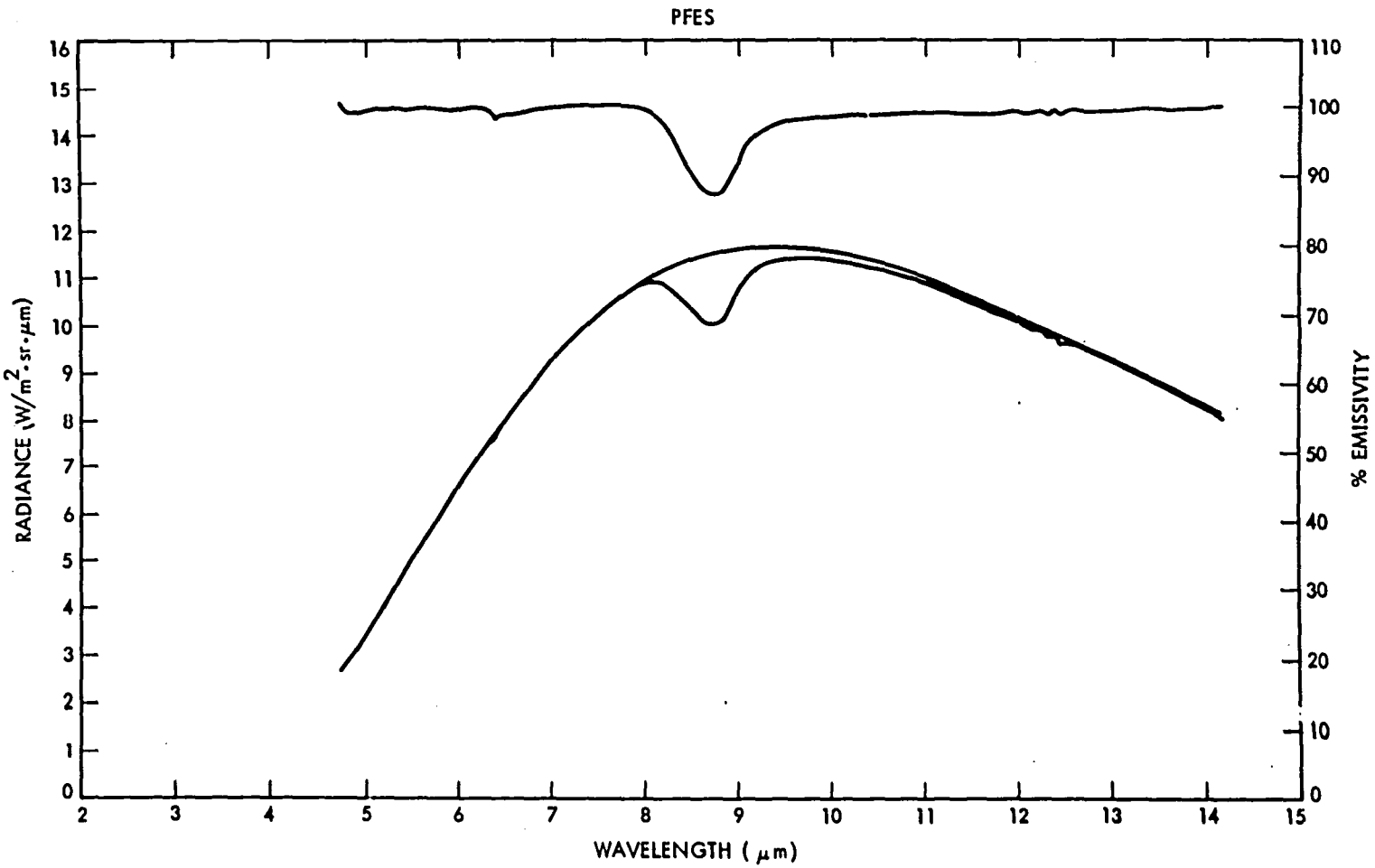

Figure 8-1. Description: Gypsum-Bearing Soil
Location of Site: Riverton, Wyoming
Date: 27 July 1984
Blackbody Temperature: 36.3 Degrees Celsius

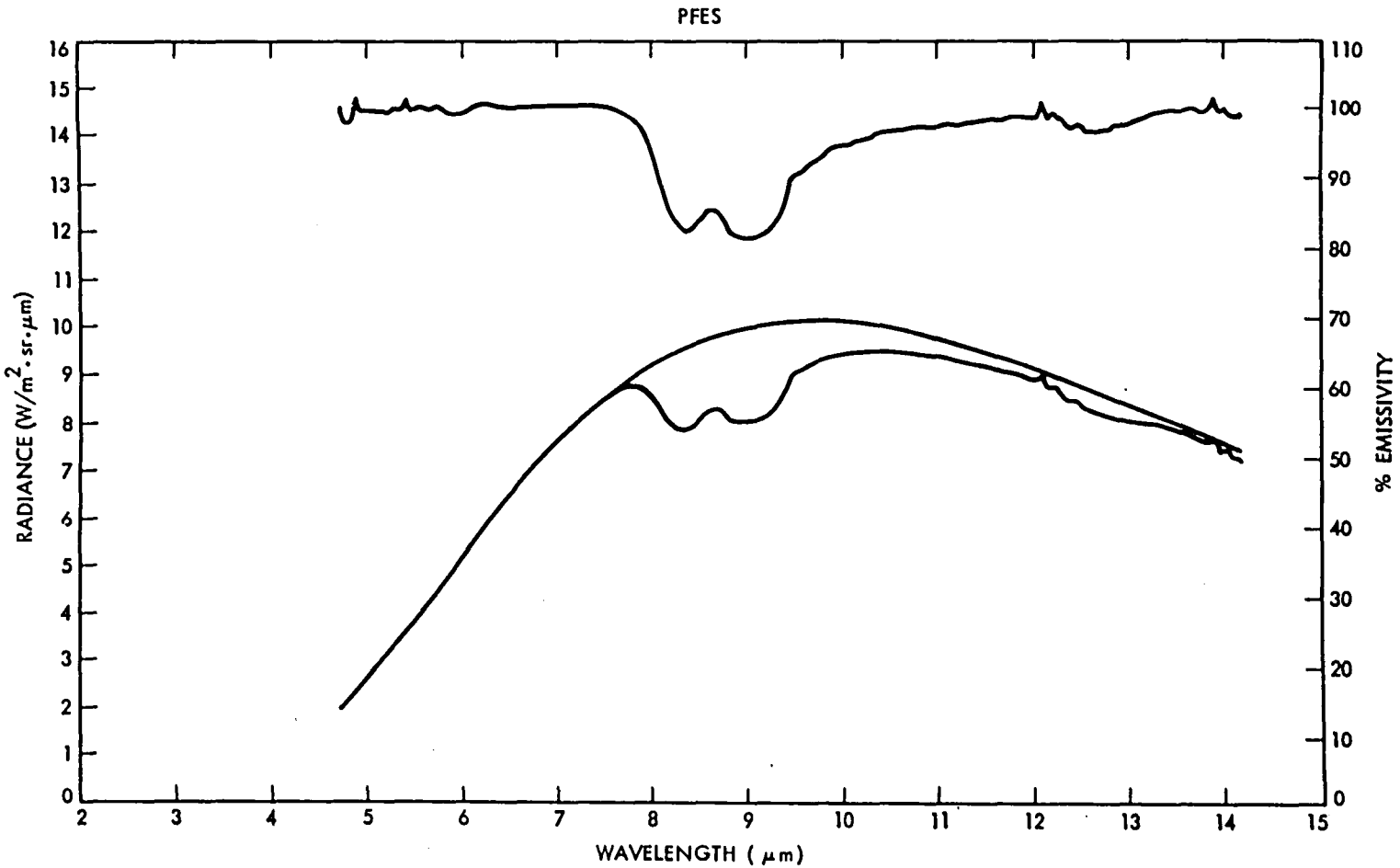

Figure 8-2. Description: Quartzite Outcrop
Location of Site: Death Valley, California
Date: 19 November 1984
Blackbody Temperature: 27.3 Degrees Celsius

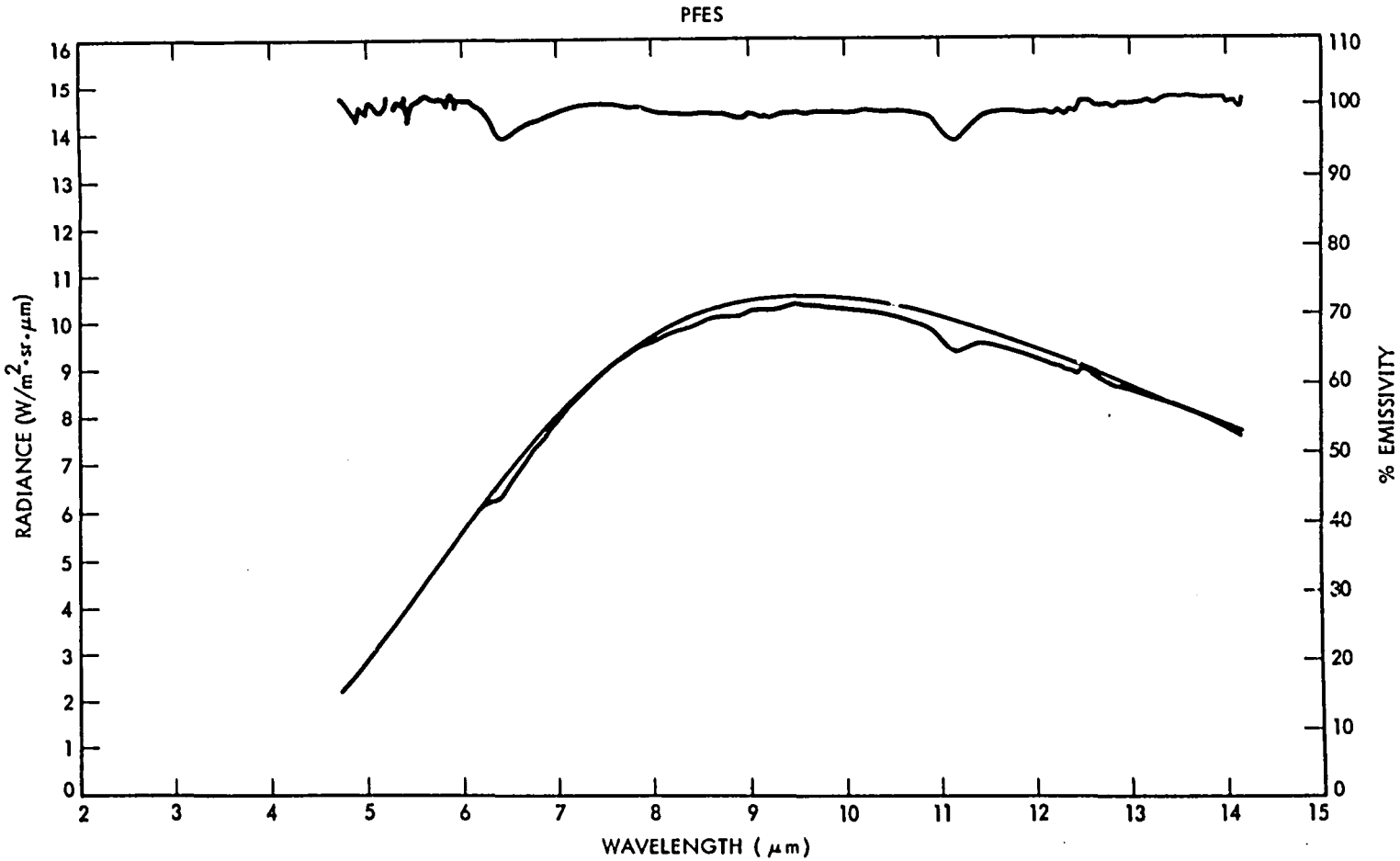

Figure 8-3. Description: Dolomite Boulder
Location of Site; Death Valley, California
Date: 19 November 1984
Blackbody Temperature: 29.7 Degrees Celsius

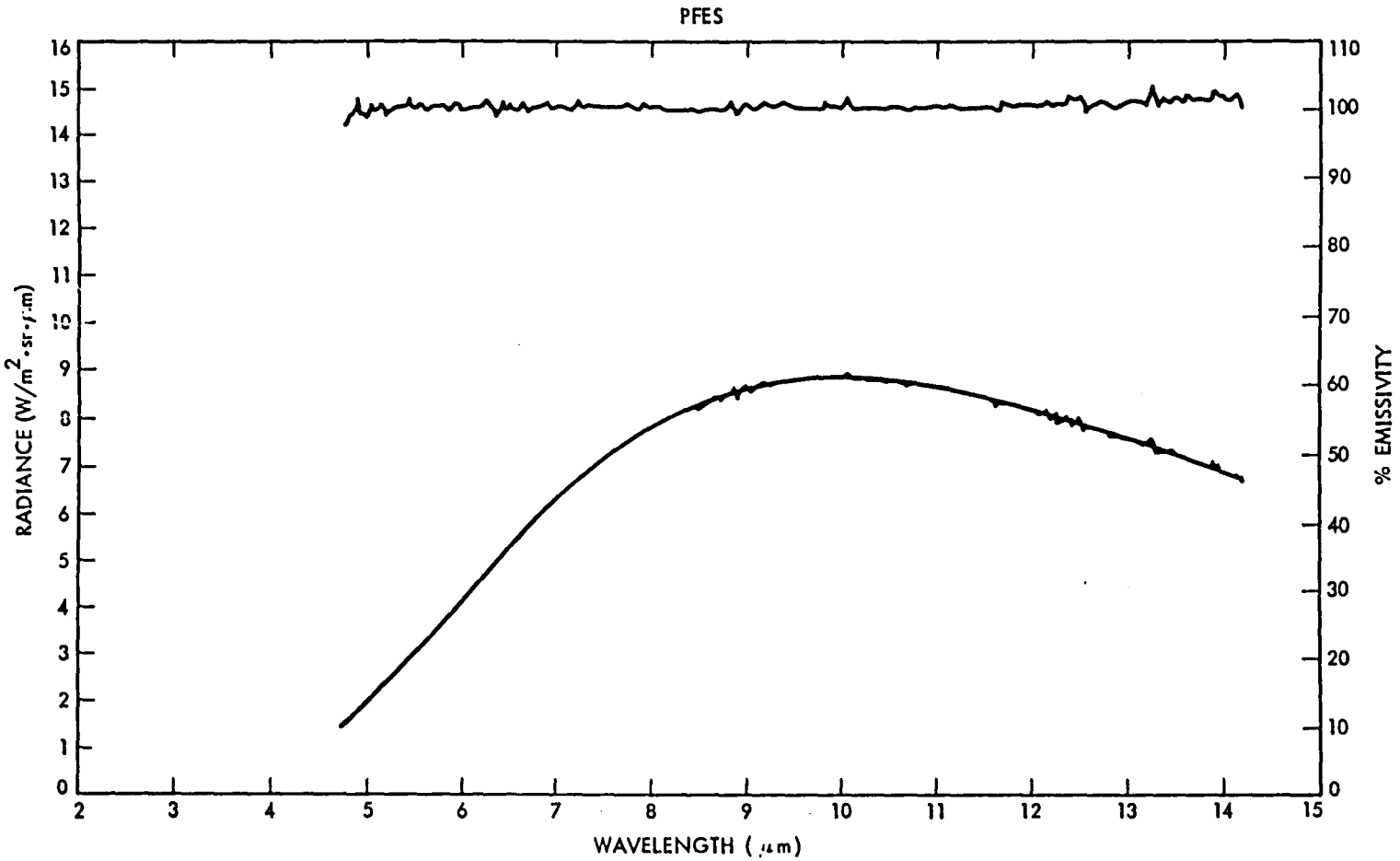

Figure 8-4. Description: Desert Holly Bush
Location of Site: Death Valley, California
Date: 22 January 1985
Blackbody Temperature: 19.7 Degrees Celsius

SECTION 9

SUMMARY

The Portable Field Emission Spectrometer (PFES) is an instrument capable of characterizing the spectral nature of the Earth's surface in the thermal infrared. It can also be used to measure the temperatures of emitting surfaces provided the emissivity is known. The system is fully portable and has, on a number of occasions, been carried several miles from the nearest road over rough terrain to collect data at remote sites. We think this instrument fills a very important niche among the tools of geologic remote sensing.

SECTION 10

REFERENCES

1-1 Kahle, Anne B. and Goetz, Alexander F. H., Mineralogic Information from a New Airborne Thermal Infrared Multispectral Scanner, Science, 222, 24-27, 1983

1-2 Goetz, A. F. H., Billingsly, F. C., Gillespie, A. R., Abrams, M. J. Squires, R. L., Shoemaker, E. M., Lucchitti, I., and Elston, D. P., Applications of ERTS Image Processing to Regional Geologic Problems and Geologic Mapping in Northern Arizona, Jet Propulsion Laboratory Technical Report. 32-1597, Pasadena, Cal., 1975

6-1 Conel, J. E., Infrared Emissivities of Silicates: Experimental Results and a Cloudy Atmosphere Model of Spectral Emission for Condensed Particulate Mediums, J. Geophysic. Res., 74, 1614-1634, 1969

8-1 Lyon, R. J. P., Evaluation of Infrared Spectrophotometry for Compositional Analysis of Lunar and Planetary Soils, Part II: Rough and Powdered Surfaces, NASA Contractor Report CR-100, 172 pp., Stanford University, Stanford, California, 1964

8-2 Lunt, G. R. and Salisbury, J. W., Mid-infrared Spectral Behavior of Metamorphic Rocks, AFCRL-TR-76-0003, Air Force Cambridge Research Laboratory, Hanscom, Massachusetts, 1976

8-3 Hunt, G. R., Electromagnetic Radiation: the Communication Link in Remote Sensing, in Siegal, B. S. and Gillespie, A. R., Eds., Remote Sensing Geology, John Wiley & Sons, New York, New York, 1980

End of Document